ChemComm

enantio-Enriched CPL-active helicene–bipyridine–rhenium complexes†

Nidal Saleh,[a] Monika Srebro,[b] Thibault Reynaldo,[a] Nicolas Vanthuyne,[c] Loïc Toupet,[a] Victoria Y. Chang,[d] Gilles Muller,[d] J. A. Gareth Williams,[e] Christian Roussel,[c] Jochen Autschbach*[f] and Jeanne Crassous*[a]

The incorporation of a rhenium atom within an extended helical π-conjugated bi-pyridine system impacts the chiroptical and photophysical properties of the resulting neutral or cationic complexes, leading to the first examples of rhenium-based phosphors that exhibit circularly polarized luminescence.

2,2′-Bipyridine (bipy) derivatives are widely used N,N'-bidentate ligands in coordination chemistry, giving access to a great variety of complexes.[1] The luminescence properties of d^6 transition metal polypyridyl complexes have been increasingly studied for the development of new metal-based luminescent materials and sensing probes.[2] Among them, $[Re(N,N')(CO)_3X]^{0/+}$ complexes (X = halide, pyridyl (py) or isocyanide (CNR)) exhibit room-temperature (RT) phosphorescence from triplet metal-to-ligand (ML) and/or intraligand charge-transfer (ILCT) states.[3,4] Such d^6-complexes find applications as electroswitchable emissive systems,[5a] cellular imaging agents,[5b,c] chromophores for photoredox chemistry,[5d] etc. It would therefore be of great interest to develop chiral analogues[6] in order to benefit from the chiral version of emission, namely circularly polarized luminescence (CPL) which may potentially be used in cryptography or for 3D-displays.[7,8]

In this communication, we describe the synthesis of tricarbonyl Re^I complexes of general formula $[Re(N^\wedge N')(CO)_3X]^{0/+}$ (X = halide, pyridyl or isocyanide) with $N^\wedge N'$ being either achiral 3-(2-pyridyl)-4-aza[4]-helicene (**1a**) or chiral 3-(2-pyridyl)-4-aza[6]-helicene

[a] Institut des Sciences Chimiques de Rennes, UMR 6226, Institut de Physique de Rennes, UMR 6251, Campus de Beaulieu, CNRS-Université de Rennes 1, 35042 Rennes Cedex, France. E-mail: jeanne.crassous@univ-rennes1.fr

[b] Faculty of Chemistry, Jagiellonian University, 30-060 Krakow, Poland

[c] Aix Marseille Université, Centrale Marseille, CNRS, iSm2 UMR 7313, 13397, Marseille, France

[d] Department of Chemistry, San José State University, San José, CA 95192-0101, USA

[e] Department of Chemistry, University of Durham, Durham, DH1 3LE, UK

[f] Department of Chemistry, University at Buffalo, State University of New York, Buffalo, NY 14260, USA. E-mail: jochena@buffalo.edu

† Electronic supplementary information (ESI) available: Synthetic, spectroscopic and computational details. CCDC 857156, 939180 and 942143. For ESI and crystallographic data in CIF or other electronic format see DOI: 10.1039/c5cc00453e

Scheme 1 Synthesis of rhenium complexes **2a–4a** and enantio-enriched (M,A_{Re})-**2b¹**, (M,C_{Re})-**2b²** and $(M,A_{Re}*)$-**3b¹,²** from respectively [4]helicene-bipy, **1a** and M-[6]helicene-bipy, M-**1b**. (i) $Re(CO)_5Cl$, toluene, reflux; (ii) AgOTf, EtOH/THF, then 2,6-dimethylphenyl isocyanide, THF, NH_4PF_6, 75–80%; (iii) $AgBF_4$, CH_3CN, reflux then pyridine, THF, 80%. X-ray structures of racemic **2b²**, **3a** and **4a** (only (M,C^{Re}) stereoisomers are shown).[10]

(M- and P-**1b**) (Scheme 1). The stereochemical features of these novel d^6-complexes are presented in detail. The chiroptical properties of enantio-enriched samples and the non-polarized and circularly polarized phosphorescence were measured experimentally and analyzed using quantum-chemical calculations.

Re^I-complex **2a** was obtained in 85% yield as a yellow-orange precipitate upon refluxing a solution of **1a**[8g] and $Re(CO)_5Cl$ in toluene for 5 hours (Scheme 1). It was fully characterized by multinuclear NMR spectroscopy (one set of peaks), by elemental analysis, UV-vis and emission spectroscopies. As compared to ligand **1a**, the ^1H NMR spectrum of **2a** shows strongly deshielded signals (except for H^2, H^{12} and $H^{6'}$) with $\Delta\delta$ up to +0.8 ppm for H^5 (see ESI†). The UV-vis spectrum of ligand **1a** in CH_2Cl_2 displays a strong band at 295 nm ($\varepsilon > 50 \times 10^3$ M^{-1} cm^{-1}), accompanied by several structured bands of lower intensity between 300 and 400 nm. Meanwhile, complex **2a** shows several absorption bands between 230 and 370 nm ($\varepsilon \sim 30–43 \times 10^3$ M^{-1} cm^{-1}) that can be assigned to intraligand π–π* transitions and a broad, low-energy absorption band between 370 and 480 nm ($\lambda_{max} = 398$ nm, $\varepsilon = 12\,700$ M^{-1} cm^{-1})

This journal is © The Royal Society of Chemistry 2015

related to the incorporation of the Re^I metal and predominantly assigned as ILCT with contributions of MLCT character (*vide infra*). The absorption maximum at 398 nm appears red-shifted compared to the corresponding band in $Re(2,2'\text{-bpy})(CO)_3Cl$[3f] (350 nm) indicating extended π-conjugation.

Re^I complex **2a** is red-phosphorescent in CH_2Cl_2 at RT (λ_{max}^{phos} = 678 nm, ϕ = 0.11%, τ = 25 ns, see ESI†). The phosphorescence originates from the triplet charge-transfer state. It is facilitated by spin–orbit coupling at the rhenium heavy atom and bathochromically shifted compared to that of $Re(2,2'\text{-bpy})(CO)_3Cl$ (λ_{max}^{phos} = 610 nm).[3f] At 77 K, the phosphorescence of **2a** is significantly shifted to shorter wavelengths (λ_{max}^{phos} = 550 nm, τ = 7.9 μs). Such a hypsochromic shift is usually explained by inversion of the energies of $^3\pi-\pi^*$ and ^{3}MLCT triplet states and/or by rigidification of the system.[3] Note that as usual in this class of complexes, the quantum yield at RT is rather low.[3] In comparison, charged complexes of formula $[Re(N^\wedge N')(CO)_3py]^+$ or $[Re(N^\wedge N')(CO)_3CNR]^+$ typically display superior luminescence efficiency due to a stronger ligand field. For this reason, complexes **3a** and **4a** were prepared in good yields from **1a**, according to Scheme 1. They were fully characterized by multinuclear NMR spectroscopy, elemental analysis, UV-vis spectroscopy, emission and X-ray crystallography. The **3a** and **4a** compounds crystallize in Fdd2 and $P2_1/n$ centrosymmetric space groups respectively (Scheme 1). At this stage, it is worth noting that complexes **2a–4a** are chiral at the rhenium centre,‡[9] since the Re atoms adopt a slightly distorted octahedral geometry, with three carbonyl groups being *fac*-oriented around the Re^I, as classically seen in such rhenium(I) tricarbonyl diimine complexes.[3] The equatorial planes are defined by the chelate bipyridine ligand and two *trans* carbonyls. A third carbonyl and either the chlorine, the isocyanide or the pyridine are placed in the apical positions. Note that in structures **3a,4a** the [4]helicene-bpy ligand exhibits a helicity angle (defined as angle between the terminal rings of the helicene moiety) of ~35° and the cyanide and pyridine ligand are directed towards it, thus defining the (P,A^{Re}) and (M,C^{Re}) stereochemistry.[10] However, in solution, the helicene is not configurationally stable, and the Re center readily epimerizes (*vide infra*). As expected, the charged complexes displayed improved photophysical properties with similar UV-visible and emission spectra as for **2a** (see ESI†), but with higher quantum yields (**3a**: 16%; **4a**: 8.3%). These results prompted us to prepare tricarbonylrhenium(I) complexes bearing a configurationally stable enantiopure [6]helicene-bipy ligand.

Racemic **1b** was reacted with $Re(CO)_5Cl$ in refluxing toluene for 5 hours, yielding after purification by column chromatography two distinct diastereomeric Re(I) complexes (**2b¹** and **2b²**, with 28% and 52% yields, respectively) as evidenced by ^1H and ^{13}C NMR spectroscopy (for example H^{15}: 6.7 ppm for **2b¹** and 6.9 ppm for **2b²**, see ESI†). Complex **2b²** crystallizes in a centrosymmetric space group ($P2_1/C$) in which two enantiomeric structures, namely (M,C^{Re})- and (P,A^{Re})-**2b²** are present (Scheme 1).[10] Note that a substantial distortion results from the bite angles between the chelating N atoms of the helicenic ligand, the rhenium centre and the chloride ligand ranging between 82.6 and 84.3°. In complex **2b²** the chlorine atom is directed towards the helicene moiety, whereas it directs outwards from the helicene core in the enantiomeric complexes (M,A^{Re}) and

(P,C^{Re})-**2b¹**. The helicity of the aza[6]helicene moiety ranges between 47.0–66.2°, which is typical for aza[6]helicene derivatives (58° for carbo[6]helicene).[8] Finally, complexation with Re affords an extended π-conjugation over the whole molecule, as evidenced by the small NCCN dihedral angles between the two chelating pyridine moieties (−3.1–6.0°). The extended π-conjugation and the metal-ligand interaction are evidenced by UV-vis spectroscopy since **2b**^{1,2} display similar UV-vis spectra with a set of several bands between 330 and 450 nm (ε ~ 7–25 × 10^3 M^{-1} cm^{-1}) that are bathochromically shifted and more intense compared to ligand **1b**, together with a very weak band observed between 450 and 500 nm (see Fig. S21, ESI†). Calculations at the BHLYP/SV(P) level with a continuum solvent model for CH_2Cl_2 reproduce well these data and show that the low-energy band of the spectrum is dominated by an ILCT transition, π(helicene) → π*($N^\wedge N'$), while the medium-energy bands are mostly π-to-π* 'CT-like' transitions localized within the helicene moiety (*vide infra*, ESI†) in agreement with assignments of absorption spectra of related rhenium(I) systems, in particular for complexes with large π-conjugated ligands.[4c–e] The overall contribution of the Re orbitals is low, meaning that the primary effect of the metal is to rigidify the system and induce strong charge transfer from the helical π-system to the bipy $N^\wedge N'$ part of the ligand. The simulated spectral shapes and band positions agree well with experiment. It is possible, though, that the overall involvement of Re orbitals in the absorption transitions is somewhat underestimated by the BHLYP functional (*vide infra*). Re^I complexes **2b**^{1,2} are red-phosphorescent emitters in CH_2Cl_2 at RT (**2b¹**: λ_{max}^{phos} = 680 nm, ϕ = 0.13%, τ = 27 ns; **2b²**: λ_{max}^{phos} = 673 nm, ϕ = 0.16%, τ = 33 ns; for details see ESI†). At 77 K, these complexes display phosphorescence at shorter wavelengths (**2b¹**: λ_{max}^{phos} = 560 nm, τ = 46 μs; **2b²**: λ_{max}^{phos} = 554 nm, τ = 43 μs) (*vide supra*). Note that the emission properties of diastereomers **2b**^{1,2} are only slightly different and (for τ and ϕ) within the uncertainty in the measurements (see ESI†).

Enantiopure complexes (M,A^{Re})-**2b¹** and (M,C^{Re})-**2b²** were then prepared from enantiopure M-**1b** (their mirror-images (P,C^{Re})-**2b¹** and (P,A^{Re})-**2b²** from P-**1b**). Enantiopure complexes **2b**^{1,2} display similar molar rotation (MR) values to **1b** in CH_2Cl_2 {(P,C^{Re})-(+)-**2b¹**: $[\phi]_D^{23}$ = +9260 degree cm^2 $dmol^{-1}$ (±5%), calc. BHLYP +12721; (P,A^{Re})-(+)-**2b²**: $[\phi]_D^{23}$ = +10 260 (±5%), calc. BHLYP +11 888; P-(+)-**1b**:[8g] $[\phi]_D^{23}$ = +12 000 (±5%), calc. BHLYP +14176, see ESI†}. The ECD spectrum of P-**2b¹** shows a strong negative band around 261 nm ($\Delta\varepsilon$ = −114 M^{-1} cm^{-1}) and strong positive ones at 350 (+81 M^{-1} cm^{-1}) and 368 nm (+76 M^{-1} cm^{-1}) accompanied by weaker bands between 380 and 450 nm (20–40 M^{-1} cm^{-1}) and an even weaker one around 480 nm but of opposite sign ($\Delta\varepsilon$ ~ −0.6 M^{-1} cm^{-1}). Diastereomeric complex (P,A^{Re})-(+)-**2b²** exhibits the same ECD active bands as **2b¹** but they are more intense. A comparison with experimental ECD of **1b** enantiomers is displayed in Fig. 1. The calculated spectra of **2b**^{1,2} (BHLYP/SV(P) with a continuum solvent model for CH_2Cl_2) qualitatively agree well with the experimental results (Fig. 3 and Fig. S5, ESI†). A detailed analysis of dominant excitations in the low- and medium-energy parts of the simulated spectra of **2b**^{1,2} indicates that the low-energy tail of the first positive ECD band is caused by excitation no. 1 calculated at E = 3.3 eV (375 nm). The excitation can be assigned as a π–π* ILCT transition involving
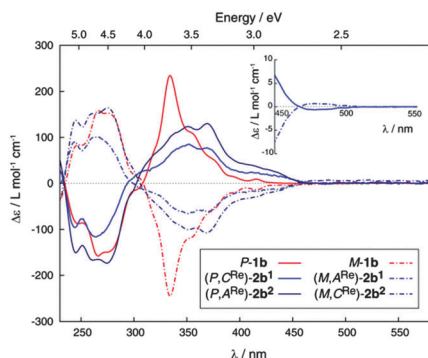
Fig. 1 Experimental CD spectra of enantiopure M-(−)-(dotted red) and P-(+)-**1b** (plain red) and enantiopure Re[I] complexes (M,A^{Re})-(−)-**2b^1** and (P,C^{Re})-(+)-**2b^1** (light blue) and (M,C^{Re})-(−)-**2b^2** and (P,A^{Re})-(+)-**2b^2** (dark blue). Inset: CD spectra of (−)- and (+)-**2b^1** between 450–550 nm.

the helicene-centered HOMO (H), H − 1, and the bipyridine N^N′-centered LUMO (L), for example for **2b^1**: H–L 51% and H − 1–L 18% (see Fig. 3 and ESI†). The next dominant **2b^{1,2}** excitation is no. 5 calculated at $E = 3.8$ eV (330 nm) with the strongest rotatory strength. It involves two main contributions from π and π^* orbital pairs localized mostly in the helicene moiety: H–L + 1 and H − 1–L + 1 (respectively 43% and 25% for **2b^1**). The excitation reveals partial CT character.

A novel aspect of these rhenium(I) helicene-based complexes is that they are CPL active (Fig. 2, top panels).[7,8] To the best of our knowledge, these are the first examples of CPL-active phosphorescent rhenium complexes. Indeed phosphorescent (P,A^{Re}) and (M,C^{Re})-**2b^2** enantiomers displayed mirror-imaged CPL spectra (Fig. 2) with opposite g_{lum} values ((P,A^{Re})-**2b^2**: $+3.1 \times 10^{-3}$ and (M,C^{Re})-**2b^2**: -2.8×10^{-3}) around the emission maximum (~ 670 nm). These values are of the same order as for the **1b** ligand enantiomers ($g_{lum} \sim \pm 10^{-3}$) but lower than those of previously published platina[6]helicenes ($g_{lum} \sim \pm 10^{-2}$),[8e] because Re orbitals are less involved in the helical π-system of the molecule (*vide supra*).

In order to improve the efficiency of the chiroptical and photophysical properties, tricarbonyl-isocyanide-helicene-bipy-Re[I] complex
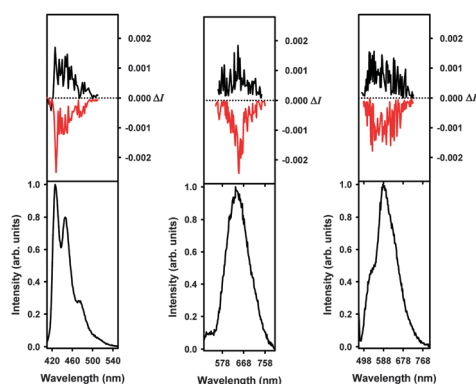
M-**3b** was prepared (see Scheme 1) in 75% yield from either (M,A^{Re})-(−)-**2b^1** or (M,C^{Re})-(−)-**2b^2**. In this complex, the Re center appeared labile and **3b** was obtained as a mixture of (M,A^{Re})-**3b^1** and (M,C^{Re})-**3b^2** as observed by ^{1}H and ^{13}C NMR spectroscopy (diastereomeric ratio 50:50, see Fig. S27, ESI†) regardless of the diastereomeric purity of the starting compound used (either **2b^1** or **2b^2** or **2b^{1,2}**). Nevertheless, as expected, this diastereomeric mixture exhibited an improved quantum yield ($\lambda_{max}^{phos} = 598$ nm, $\phi = 6\%$, $\tau = 79$ μs; see ESI†) as compared to **2b^{1,2}**. The UV-vis spectrum of **3b^{1,2}** displays the same shape as **2b^1** (see Fig. S21, ESI†). Compared to (P,C^{Re})-**2b^1** and (P,A^{Re})-**2b^2**, cationic diastereomeric mixture of Re[I] complexes P-**3b^{1,2}** demonstrates an additional positive CD-active band around 450 nm ($\Delta\varepsilon = 17.5$ M^{-1} cm^{-1}). As for **2b^{1,2}**, this latter band does not involve the Re center, but corresponds to the H–L transition ($>74\%$) with strong charge transfer from the π-helicene to the bipy moiety, as evidenced by BHLYP calculations (see Fig. 3 and ESI†). The appearance of the 450 nm band is caused mainly by a bathochromic shift of the first singlet excitation. This charge-transfer excitation is likely responsible for the enhancement of molar rotations as compared to **2b^{1,2}** {(P,AC^{Re})-(+)-**3b**: $[\phi]_D^{23} = 15\,040$ degree cm^2 dmol^{-1} ($\pm 5\%$) ($C = 8.8 \times 10^{-5}$ M, CH$_2$Cl$_2$); (M,AC^{Re})-(−)-**3b**: $[\phi]_D^{23} = -14\,230$ ($\pm 5\%$) ($C = 9.7 \times 10^{-5}$ M, CH$_2$Cl$_2$); calc. BHLYP Boltzmann average for **3b^{1,2}** conformers is $+14\,034$ degree cm^2 dmol^{-1} for the P-isomers, see ESI†}.

Quantum-chemical calculations of luminescence properties have been performed for **2b^{1,2}** and **3b^{1,2}**. The results support the experimental assignments: The energies of $T_1 \rightarrow S_0$ phosphorescence transitions (~ 2.1 eV) are similar for both **2b^{1,2}** and **3b^{1,2}** and agree fairly well with the experimental data (Table S5, ESI†). An overestimation of the calculated *versus* measured energies is consistent with a blue-shift of calculated **2b^{1,2}** and **3b^{1,2}** absorption and CD spectra. The emission energies from spin–orbit (SO) calculations agree with non-SO calculations but the former allow predictions of the phosphorescence lifetimes. Application of the BHLYP functional along with the Tamm-Dancoff approximation (see ESI†) resulted in much too high emission lifetimes (Table S6, ESI†). As the involvement of Re orbitals facilitates the formally spin-forbidden $T_1 \rightarrow S_0$ phosphorescence transitions *via* spin–orbit coupling, decreasing the corresponding lifetimes, too high τ calculated with BHLYP may indicate that the metal orbital contributions
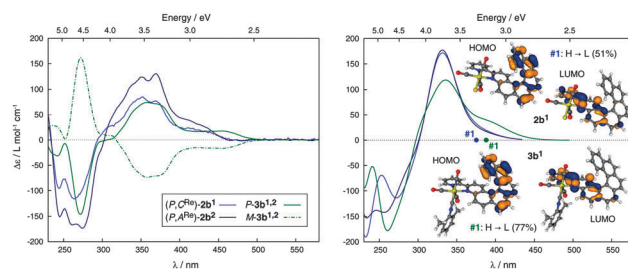

Fig. 2 CPL (upper curves within each panel) and total luminescence (lower curves within each panel) spectra of M-(−)-**1b** (left red), P-(+)-**1b** (left black), M-(−)-**2b^2** (middle red), P-(+)-**2b^2** (middle black), M-(−)-**3b^{1,2}** (right red), P-(+)-**3b^{1,2}** (right black) in degassed CH$_2$Cl$_2$ solution (1 mM) at 295 K, upon excitation at 400, 456–461, and 458–468 nm, respectively.

Fig. 3 Left: experimental CD spectra of enantiopure complexes (P,C^{Re})-(+)-**2b^1** (light blue), (P,A^{Re})-(+)-**2b^2** (dark blue) and of (M,CA^{Re})-(−)-**3b^{1,2}** (dotted green) and (P,CA^{Re})-(+)-**3b^{1,2}** (plain green). Right: calculated CD spectra of (P,C^{Re})-**2b^1**, and (P,A^{Re})-**2b^2** and Boltzmann-averaged spectrum for P-**3b^{1,2}** conformers. No spectral shifts were applied. View of HOMO and LUMO of **2b^1** and **3b^1** (0.04 au). First excitation energies indicated by dots on the abscissa.

to the frontier MOs are somewhat too small. The performance of a given functional for singlet *vs.* triplet transitions is not necessarily the same. When applying a computational protocol for emission lifetimes devised recently by Mori *et al.*[11] for organometallic complexes (full TDDFT with the B3LYP functional), a dramatic improvement of the lifetimes and some lowering of the emission energies (to $\sim$1.9 eV) was obtained (Table S7, ESI†), which correlates with increased participation of Re orbitals in the frontier MOs at the triplet geometries. Notably the experimental trend of an increase in emission lifetime by roughly an order of magnitude when going from $2b^{1,2}$ to $3b^{1,2}$ is correctly reproduced with B3LYP and qualitatively consistent with lesser metal orbital participation (lesser MLCT character) in the T_1 emission transitions for $3b^{1,2}$ as compared to $2b^{1,2}$ (see ESI†).§[4a,b]

Finally, mirror-imaged CPL spectra were obtained in CH_2Cl_2 for (M,AC^{Re})-$3b^{1,2}$ and (P,AC^{Re})-$3b^{1,2}$ (Fig. 2) with respective g_{lum} values of -0.0015 and $+0.0013$. Overall, cationic Re^I complexes display similar CPL characteristics as neutral ones, but combined with a higher quantum yield, the polarized emitted light is stronger. Although the Re d orbitals are not strongly involved in the electronic π-systems of these novel metallo-helicenes, the metal helps to increase the π-conjugation pathway and promotes charge-transfer excitations within the π-helical ligand. In addition, the presence of the rhenium heavy atom makes these complexes chiral phosphors with unprecedented CPL activity.

Notes and references

‡ Note that enantiopure (+) and (−) complexes (**1a**)Re(CO)$_3$Br were prepared by chiral HPLC and they displayed very weak CD activity ($\Delta\varepsilon_{max}$ = 20 M^{-1} cm^{-1}, see Fig. S23, ESI†).
§ The direct comparison between experimental and calculated lifetimes must be treated with some caution, as the former are also affected by non-radiative decay pathways, which may be non-negligible even at 77 K. We assume that the non-radiative decay rates for the complexes are similar under these conditions.

1 (a) G. Chelucci and R. P. Thummel, *Chem. Rev.*, 2002, **102**, 3129; (b) H.-L. Kwong, H.-L. Yeung, C.-T. Yeung, W.-S. Lee, C.-S. Lee and W.-L. Wong, *Coord. Chem. Rev.*, 2007, **251**, 2188.
2 H. Le Bozec and V. Guerchais, *Molecular Organometallic Materials for Optics*, Topics in Organometallic Chemistry series, Springer, 2009.
3 (a) K. K.-W. Lo, M.-W. Louie and K. Y. Zhang, *Coord. Chem. Rev.*, 2010, **254**, 2603; (b) V. W.-W. Yam and K. M.-C. Wong, *Chem. Commun.*, 2011, **47**, 11579; (c) C.-C. Ko, A. W.-Y. Cheung, L. T.-L. Lo, J. W.-K. Siu, C.-O. Ng and S.-M. Yiu, *Coord. Chem. Rev.*, 2012, **256**, 1546; (d) M. Panigati, M. Mauro, D. Donghi, P. Mercandelli, P. Mussini, L. de Cola and G. D'Alfonso, *Coord. Chem. Rev.*, 2012, **256**, 1621; (e) A. J. Lee, *Chem. Rev.*, 1987, **87**, 711; (f) M. Wrighton and D. L. Morse, *J. Am. Chem. Soc.*, 1974, **96**, 998.
4 (a) M. K. Kuimova, W. Z. Alsindi, J. Dyer, D. C. Grills, O. S. Jina, P. Matousek, A. W. Parker, P. Portius, X. Z. Sun, M. Towrie, C. Wilson, J. Yang and M. W. George, *Dalton Trans.*, 2003, 3996; (b) H. van der Salm, M. G. Fraser, R. Horvath, S. A. Cameron, J. E. Barnsley, X.-Z. Sun, M. W. George and K. C. Gordon, *Inorg. Chem.*, 2014, **53**, 3126; (c) H.-J. Nie, X. Chen, C.-J. Yao, Y.-W. Zhong, G. R. Hutchison and J. Yao, *Chem. – Eur. J.*, 2012, **18**, 14497; (d) T. Yu, D. P.-K. Tsang, V. K.-M. Au, W. H. Lam, M.-Y. Chan and V. W.-W. Yam, *Chem. – Eur. J.*, 2013, **19**, 13418; (e) R. Horvath, M. G. Fraser, S. A. Cameron, A. G. Blackman, P. Wagner, D. L. Officer and K. C. Gordon, *Inorg. Chem.*, 2013, **52**, 1304.
5 Selected: (a) K. M. C. Wong, S. C. F. Lam, C. C. Ko, N. Y. Zhu, V. W.-W. Yam, S. Roue, C. Lapinte, S. Fathallah, K. Costuas, S. Kahlal and J.-F. Halet, *Inorg. Chem.*, 2003, **42**, 7086; (b) A. W.-T. Choi, V. M.-W. Yim, H.-W. Liu and K. K.-W. Lo, *Chem. – Eur. J.*, 2014, **20**, 9633; (c) S. Clède, F. Lambert, C. Sandt, Z. Gueroui, M. Réfrégiers, M.-A. Plamont, P. Dumas, A. Vessières and C. Policar, *Chem. Commun.*, 2012, **48**, 7729; (d) H. Tsubaki, A. Sekine, Y. Ohashi, K. Koike, H. Takeda and O. Ishitani, *J. Am. Chem. Soc.*, 2005, **127**, 15544.
6 (a) Y. H. Zhou, J. Li, T. Wu, X. P. Zhao, Q. L. Xu, X. L. Li, M. B. Yu, L. L. Wang, P. Sun and Y. X. Zheng, *Inorg. Chem. Commun.*, 2013, **29**, 18; (b) M. Q. Sans and P. Belser, *Coord. Chem. Rev.*, 2002, **229**, 59.
7 H. Maeda and Y. Bando, *Pure Appl. Chem.*, 2013, **85**, 1967.
8 Selected examples of CPL active helicenes: (a) J. E. Field, G. Muller, J. P. Riehl and D. Venkataraman, *J. Am. Chem. Soc.*, 2003, **125**, 11808; (b) Y. Sawada, S. Furumi, A. Takai, M. Takeuchi, K. Noguchi and K. Tanaka, *J. Am. Chem. Soc.*, 2012, **134**, 4080; (c) K. E. S. Phillips, T. J. Katz, S. Jockusch, A. J. Lovinger and N. J. Turro, *J. Am. Chem. Soc.*, 2001, **123**, 11899; (d) T. Kaseyama, S. Furumi, X. Zhang, K. Tanaka and M. Takeuchi, *Angew. Chem., Int. Ed.*, 2011, **50**, 3684; (e) C. Shen, E. Anger, M. Srebro, N. Vanthuyne, K. K. Deol, T. D. Jefferson Jr., G. Muller, J. A. G. Williams, L. Toupet, C. Roussel, J. Autschbach, R. Réau and J. Crassous, *Chem. Sci.*, 2014, **5**, 1915; (f) K. Nakamura, S. Furumi, M. Takeuchi, T. Shibuya and K. Tanaka, *J. Am. Chem. Soc.*, 2014, **136**, 5555; (g) N. Saleh, B. Moore, II, M. Srebro, N. Vanthuyne, L. Toupet, J. A. G. Williams, C. Roussel, K. K. Deol, G. Muller, J. Autschbach and J. Crassous, *Chem. – Eur. J.*, 2015, **21**, 1673.
9 For enantiopure "chiral at rhenium" complexes see: (a) S. J. Lee and W. Lin, *J. Am. Chem. Soc.*, 2002, **124**, 4554; (b) F. Bock, F. Fischer and W. A. Schenk, *J. Am. Chem. Soc.*, 2006, **128**, 68; (c) J.-D. Chen and F. A. Cotton, *J. Am. Chem. Soc.*, 1991, **113**, 2509; (d) J. H. Merrifield, C. E. Strouse and J. A. Gladysz, *Organometallics*, 1982, **1**, 1204; (e) W. E. Buhro, A. Wong, J. H. Merrifield, G.-Y. Lin, A. C. Constable and J. A. Gladysz, *Organometallics*, 1983, **2**, 1852; (f) P. R. Lassen, L. Guy, I. Karame, T. Roisnel, N. Vanthuyne, C. Roussel, X. Cao, R. Lombardi, J. Crassous, T. B. Freedman and L. A. Nafie, *Inorg. Chem.*, 2006, **45**, 10230; (g) F. De Montigny, L. Guy, G. Pilet, N. Vanthuyne, C. Roussel, R. Lombardi, T. B. Freedman, L. A. Nafie and J. Crassous, *Chem. Commun.*, 2009, 4841; (h) J. W. Faller and A. R. Lavoie, *Organometallics*, 2000, **19**, 3957; (i) W. K. Rybak, A. Skarzynska and T. Glowiak, *Angew. Chem., Int. Ed.*, 2003, **42**, 1725; (j) C. M. Alvarez, R. Carrillo, R. Garcia-Rodriguez and D. Miguel, *Chem. Commun.*, 2011, **47**, 12765; (k) E. Tazacs, A. Escande, N. Vanthuyne, C. Roussel, C. Lescop, E. Guinard, C. Latouche, A. Boucekkine, J. Crassous, R. Réau and M. Hissler, *Chem. Commun.*, 2012, **48**, 6705.
10 For the stereochemical descriptors see ESI† and A. von Zelewsky, *Stereochemistry of Coordination Compounds*, J. Wiley & Sons, Chichester, 1996.
11 K. Mori, T. P. M. Goumans, E. van Lenthe and F. Wang, *Phys. Chem. Chem. Phys.*, 2014, **16**, 14523.